

Accepted Manuscript

On the relationship between K concentration, grain size and dose in feldspar

J.-P. Buylaert, G. Újvári, A.S. Murray, R.K. Smedley, M. Kook

PII: S1350-4487(17)30869-7

DOI: [10.1016/j.radmeas.2018.06.003](https://doi.org/10.1016/j.radmeas.2018.06.003)

Reference: RM 5925

To appear in: *Radiation Measurements*

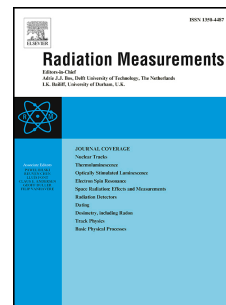
Received Date: 15 December 2017

Revised Date: 30 March 2018

Accepted Date: 2 June 2018

Please cite this article as: Buylaert, J.-P., Újvári, G., Murray, A.S., Smedley, R.K., Kook, M., On the relationship between K concentration, grain size and dose in feldspar, *Radiation Measurements* (2018), doi: [10.1016/j.radmeas.2018.06.003](https://doi.org/10.1016/j.radmeas.2018.06.003).

This is a PDF file of an unedited manuscript that has been accepted for publication. As a service to our customers we are providing this early version of the manuscript. The manuscript will undergo copyediting, typesetting, and review of the resulting proof before it is published in its final form. Please note that during the production process errors may be discovered which could affect the content, and all legal disclaimers that apply to the journal pertain.



1 On the relationship between K concentration, grain size and dose 2 in feldspar

3
4 Buylaert, J.-P.^{1,2,*}, Újvári, G.^{1,3}, Murray, A.S.², Smedley, R.K.^{4,5}, Kook, M.¹

5
6 ¹Center for Nuclear Technologies, Technical University of Denmark, DTU Risø Campus,
7 Denmark

8 ²Nordic Laboratory for Luminescence Dating, Department of Geoscience, Aarhus University,
9 Risø Campus, DK-4000 Roskilde, Denmark

10 ³Institute for Geological and Geochemical Research, Research Centre for Astronomy and
11 Earth Sciences, Hungarian Academy of Sciences, H-1112 Budapest, Hungary

12 ⁴Department of Geography and Planning, University of Liverpool, Liverpool, U.K.

13 ⁵School of Geography, Geology and the Environment, Keele University, Keele, Staffordshire,
14 U.K.

15
16 * corresponding author: jabu@dtu.dk

17 18 Abstract

19 Previous work has been unable to establish a relationship between K concentration and D_e in
20 single-grains of feldspar. Here we use four well-bleached sediments with low external dose
21 rate (typically $\leq 1.5 \text{ Gy ka}^{-1}$) to investigate this relationship. Single and multi-grain pIRIR
22 measurements and μ -XRF analyses are made on Na- and K-rich extracts; μ -XRF is directly
23 applied to grains sitting in single-grain discs to minimise uncertainty in grain identification.
24 Micro-XRF is shown to be sufficiently precise and accurate and luminescence instrument
25 reproducibility is confirmed using dose recovery measurements on heated feldspar. We are

26 again unable to establish any correlation between single-grain D_e and K concentration, even in
27 feldspar grains for which the internal dose rate should dominate. We also measure highly
28 variable Rb concentrations in these grains and are unable detect, at the single-grain level, the
29 correlation between K and Rb previously observed in multi-grain investigations.
30 Nevertheless, these results are unable to explain the lack of D_e correlation with K. Finally, we
31 investigate the dependence of D_e on grain size (isochrons). Linear correlations are observed
32 but slopes are inconsistent with model prediction. We conclude that this surprising absence of
33 the expected relationships between dose and K concentration and grain size does not arise
34 from analytical precision, incomplete bleaching, sediment mixing or fading. It appears that we
35 cannot measure feldspar doses in these samples as accurately as we thought.

36

37 Keywords: feldspar; potassium; rubidium; dose; isochron

38

39 **1. Introduction**

40 The over-dispersion in single-grain dose distributions determined in feldspar from a well-
41 bleached setting must, at least in part, arise from the grain-to-grain variation in internal dose
42 rate (dominated by stoichiometrically predicted variations in K concentration ranging from 0
43 to 14%). However, it has so far proved impossible to demonstrate this relationship
44 experimentally (e.g. Trauerstein et al., 2014; Smedley and Pearce, 2016). Such correlations
45 will not be particularly pronounced in medium to high dose rate environments where the
46 internal dose rate is only a moderate contribution to the total, and this could partly explain
47 why it has not been observed so far. However, Willerslev et al. (2007) investigated grains
48 dispersed in old Greenland ice, i.e. grains with negligible external dose rate, and were
49 nevertheless unable to demonstrate a correlation for their IR sensitive grains. In a related
50 study, Thiel et al. were also unable to demonstrate a correlation between D_e and K

51 concentration for >220 grains extracted from the bottom of the Greenland ice sheet (Christine
52 Thiel, personal communication 2017).

53

54 In contrast to these negative findings, Li et al. (2008) have been able to demonstrate at the
55 multi-grain level a clear relationship between D_e and K-feldspar grain size (and thus internal
56 dose rate) in their isochron work. Given these apparently contradictory results, here we first
57 investigate the relationship between D_e and K concentration at the single grain level in a
58 number of samples of known low external dose rate (typically $\leq 1.5 \text{ Gy ka}^{-1}$) expected to
59 contain well-bleached feldspar. We report on the precision and accuracy of our K
60 measurements using μ -XRF and the dependence of the single-grain D_e on K concentration.
61 We then re-examine the relationship of multi-grain D_e and grain-size (and so internal dose
62 rate). Finally, the relationship between Rb content and K concentration at the feldspar single-
63 grain level is investigated. The implications of our findings are discussed in the context of
64 luminescence dating of sand-sized feldspar grains.

65

66 **2. Methods**

67 *2.1. Samples*

68 This study focussed on feldspars originating from sedimentary environments of relatively low
69 external dose rate ($\leq 1.5 \text{ Gy ka}^{-1}$) so that the internal ^{40}K beta dose rate makes up a significant
70 ($\geq 30\%$) proportion of the total dose rate. Four low dose rate sand samples were chosen from
71 aeolian, beach, shallow marine and fluvial environments. The aeolian sample (178109) was a
72 carbonate-cemented stratified aeolianite from Portugal. The beach sample (178112) from
73 Skagen (Denmark) was an aeolian deposit sandwiched between two peat layers. The shallow
74 marine sample (981007) is of Eemian age and is intercalated between an early Weichselian
75 till and an early Eemian clay (Murray and Funder, 2003; Buylaert et al., 2011, 2012). A

76 sample (D38146) from an ~3 m thick last glacial Chinese loess unit with a high external dose
77 rate ($\sim 3 \text{ Gy ka}^{-1}$) (Section 4.2) was also used. In all these four cases, because of the presence
78 of sedimentary structures with the units, we can be confident that vertical mixing between
79 units of different ages is very unlikely; they are very likely to be well-bleached because of the
80 deposition environments. A fifth sample, a low dose rate fluvial sand (133311) from The
81 Netherlands was also used. Standard sample preparation techniques were applied (wet sieving
82 to $>63 \mu\text{m}$, 10% HCl, 10% H_2O_2 , 10% HF for 20-40 minutes). Hydrofluoric etching of the
83 grains is carried out to avoid the influence of coatings (e.g. Fe-oxides) and/or feldspar
84 weathering products on the chemical analyses (Section 2.3). The potassium- and sodium-
85 feldspar fractions were separated using heavy liquid (K-feldspar: $\rho < 2.58 \text{ g cm}^{-3}$; Na-
86 feldspar: $2.58 \text{ g cm}^{-3} < \rho < 2.62 \text{ g cm}^{-3}$) and then dried at $45 \text{ }^\circ\text{C}$. Quartz was isolated from the
87 $>2.62 \text{ g cm}^{-3}$ fraction by 40-60 min concentrated HF treatment. A summary of relevant quartz
88 OSL data, external dose rates and grain size ranges can be found in Supplementary Table 1.

89

90 2.2. Luminescence measurements

91 For single-grain measurements, Risø TL/OSL DA-20 readers with dual-laser single-grain
92 attachments were used (Bøtter-Jensen et al., 2003). Multi-grain measurements were carried
93 out on standard Risø TL/OSL DA-20 readers (Bøtter-Jensen et al., 2010). The IRSL and post-
94 IR IRSL signals were detected through a combination of Corning 7/59 and Schott BG39
95 filters (blue filter combination). For single-grain measurements, feldspar grains were loaded
96 in standard single-grain discs (10x10 grid, 300 μm deep and wide holes). Molybdenum cups
97 were used as a substrate for the multi-grain aliquots containing many hundreds of loose
98 feldspar grains. Grain-size-dependent beta dose rates were taken from Hansen et al. (these
99 proceedings). Post-IR IRSL signals (Thomsen et al., 2008) were measured using a post-IR
100 $\text{IR}_{50,150}$ (Madsen et al., 2011) or a post-IR IR_{290} (Thiel et al., 2011) protocol. Both for single

101 grain and multi-grain D_e measurements, first IR stimulations were made with IR LEDs for
102 200 s with the sample held at 50°C (except for sample D38146 for which it was 200°C). The
103 post-IR IR stimulation at 150°C or 290°C was done with the IR laser (1 s) in the case of
104 single grains and with IR LEDs (200 s) for multigrain aliquots. High temperature IR
105 bleaching (200 s) at the end of the SAR cycle were carried out at 200°C and 325°C using
106 LEDs for the pIRIR₁₅₀ and pIRIR₂₉₀ protocols, respectively. Fading rates (g values) were
107 measured following Auclair et al. (2003), using a SAR protocol on multi-grain aliquots
108 mounted on stainless steel cups using silicon spray.

109
110 The software package *Analyst* (version 4.31.9; Duller, 2016) was used for signal processing
111 and calculation of, D_e , $g_{2\text{days}}$ value and uncertainties. Net single-grain pIRIR signals were
112 calculated from the first 0.034 s of stimulation minus a background derived from the last
113 0.272 s of stimulation. Multi-grain IR and pIRIR signals were derived from the first 2 s and
114 the last 50 s of stimulation. Dose response curves were fitted using single saturating
115 exponential functions. Single-grain D_e values were accepted if the uncertainty on the test dose
116 signal was <10 %. We could not detect a dependence of single-grain D_e on recycling ratio,
117 indicating that the average D_e is unaffected by rejecting grains with relatively poor recycling
118 ratios (Fig. S1); this has already been shown to be true for quartz single grain OSL (Thomsen
119 et al., 2012, 2016). On average the recycling ratios are within 3% of unity (except for sample
120 981007 for which it is 8%) which we consider satisfactory. A measurement error of 2.5 %
121 was incorporated into the uncertainty on the single-grain D_e values.

122

123 2.3. Chemical analyses

124 After D_e measurement, single-grain discs were transferred directly to a Brüker M4 Tornado μ -
125 XRF instrument (beam spot size: ~25 μm , effective K, Ca sampling depth ~30 μm , Na ~5 μm)

126 to determine the Si, Al, K, Na, Ca and Rb concentrations. Calibration of the μ -XRF involved
127 three K-feldspar (JF-2, NIST SRM70a, NIM-S) and three Na-feldspar (BSC-375, AL-I, JSy-
128 1) reference materials, each of well-known chemical compositions (Jochum et al., 2005).
129 Calibration factors/equations for each element of interest were obtained by comparing
130 measured and accepted values of reference feldspars over a broad compositional range in K
131 and Na. Repeated analyses of independently known absolute feldspar standards (BCS CRM-
132 376/1, CRPG FK-N, SX 16-02 and ZK) with K concentrations between 4 and 14.2 %
133 demonstrated that the μ -XRF analyses are accurate within 0.2–0.9 %K and reproducible
134 within 0.1–0.47 %K. Rb measurements of the CRPG FK-N potassium feldspar standard
135 yielded a mean Rb concentration of 871 ppm (standard error (se)=25 ppm, n=5) to be
136 compared to the certified value of 860 ppm.

137
138 The μ -XRF analyses were restricted to pre-defined regions of each single-grain to reduce the
139 Al background from the single-grain disc to negligible levels. Analyses focussed only on
140 intact single grains, and if more than one grain was present in a hole these grains were
141 ignored. At least three randomly placed spots were measured on each grain with acquisition
142 times of 45 s using a single Rh target X-ray tube (600 μ A, 50kV) focussed to a spot size of
143 \sim 25 μ m by polycapillary lens optics. Raw analytical data were corrected off-line using
144 previously determined calibration factors (see above).

145 Subsequent to D_e measurement, multigrain aliquots were transferred to another luminescence
146 reader equipped with a Risø XRF attachment (Kook et al., 2012) and analysed for relative K,
147 Na and Ca content (e.g. Porat et al, 2015).

148

149 **3. Precision**

150 *3.1 Single-grain dose measurement*

151 The reproducibility of dose measurement was investigated using single grains. Annealed
152 (550°C /1 h) 180-212 µm K-feldspar grains of sample 178109 were loaded in 12 single grain
153 discs. One group of six discs was given a dose of 8 Gy and the other group a dose of 20 Gy
154 and both groups were measured using a pIRIR_{50,290} protocol (test dose 4 and 10 Gy,
155 respectively). The overall measured-to-given dose ratio was close to unity (1.017 ± 0.004 , n=
156 946 grains) and the associated average over-dispersion 6.2 ± 0.8 % (n=12 discs). This over-
157 dispersion has been added in quadrature to the uncertainty of all the single-grain dose
158 measurement discussed below (cf. Thomsen et al. (2005) for single grain quartz OSL D_e
159 values).

160

161 *3.2 Single-grain K measurement*

162 The precision of our µ-XRF K measurements was tested using between 3 and 7 repeat
163 measurements on selected individual grains from three samples. Figure S2a-c shows that these
164 K analyses are reproducible within each grain with an average standard deviation of 0.8 % K
165 (Fig. S2d).

166

167 **4. Results**

168 *4.1 Relationship between single-grain D_e and K concentration*

169 In a typical sediment where the average total dose rate to 200 µm K-rich feldspar grains is
170 $2.5 \text{ Gy} \cdot \text{ka}^{-1}$, calculations predict that ~30 % of this dose rate should come from ^{40}K internal to
171 the grain (assuming the usual 12.5% K concentration, Huntley and Baril, 1997). In this
172 experiment, we first measure the pIRIR D_e on a grain-by-grain basis and then the K
173 concentration in each grain. Because the grains remain in the single-grain disc and are not
174 disturbed between dose and concentration measurements, we are confident that our dose and
175 concentration measurements directly correspond to one another.

176
177 Apparent potassium concentrations in K- and Na-rich separates from 4 samples are
178 summarised in Fig. 1 and range between 0 and 16 %, with most between 10-14 %. It appears
179 that none of the Na-feldspar extracts are pure; they all contain a significant fraction of high-K
180 concentration grains. There are also some low K concentration grains in the K-rich extracts
181 for two samples (Fig. 1a,b) but these are not common. The expected relationships between
182 dose and K concentrations (dashed lines in Fig. 1) are based on the measured large aliquot
183 quartz age and predicted feldspar dose rate. None of our samples show the expected
184 relationship between D_e and K concentration, and almost all of the single-grain doses (and the
185 calculated KF CAM D_e) underestimate the expected dose (single grains of sample 981007
186 also underestimate the independent Eemian age control, Murray and Funder, 2003). It is
187 interesting to note that the synthetic aliquot data (summing all the luminescence from a single
188 grain disc) also tend to underestimate the large aliquot dose estimate for 3 out of 4 samples.
189 This may have arisen from the different experimental conditions - large aliquot pIRIR D_e 's
190 were measured using IR LEDs whereas single grains were stimulated both with IR LEDs
191 (IRSL at 50°C) and the single grain IR laser (elevated temperature). Further research is
192 needed to clarify the cause of this discrepancy.

193

194 *4.2 Multi-grain isochron*

195 An alternative approach to investigating the dependence of D_e on the K contribution to
196 internal dose rate is to measure the multi-grain K-feldspar D_e for different grain sizes and
197 construct an age isochron (Mejdahl, 1983; Li et al., 2008). Four samples (178109, 178112,
198 133311, see above, and D38146) were sieved to different grain sizes (43-63, 63-90, 90-125,
199 125-180, 180-212, 212-250, 250-300, 300-500 μm ; Table S1). The overall purity of the K-
200 rich extracts was confirmed using the multi-grain XRF-attachment on the reader (Fig.

201 2b,d,f,h). Measurements of several aliquots from individual samples give an overall standard
202 deviation of 0.30% K (this includes any natural inter-aliquot variability).

203 Isochrons of positive slopes were measured using both IR₅₀ and pIRIR signals for three
204 samples (Fig. 2a,c,e) but surprisingly for the loess sample (D38146, Fig. 2g) the slope is
205 negative. In view of this we used a dose recovery test to confirm that our chosen protocol was
206 able to measure accurately a given dose independent of grain size (data not shown). All
207 deviations from unity are <7% and do not correlate with the negative slope of the isochron.
208 There is no evidence that we can attribute the unexpected negative slope of this sample to
209 poor SAR performance.

210
211 In addition, even for the samples for which the isochrons are positive the slopes of both the
212 IR₅₀ and pIRIR data are consistently lower than expected and even the pIRIR data do not
213 predict the expected dose at 0% K. In all cases the apparent feldspar age is dependent on grain
214 size. Nevertheless it is interesting to note that the pIRIR signal measured on 200 µm grains
215 would give an age consistent with quartz for samples 178112 and D38146 (Fig. 2c,g; see also
216 Fig. 1c for sample 178112). For the other two samples the pIRIR signal would underestimate
217 at 200 µm (Fig. 2a,e, see also Fig. 1a,d).

218

219 *4.3 Single grain K / Rb ratios*

220 Warren (1978) was the first to assess the contribution of ⁸⁷Rb to the internal dose rate
221 assuming a K to Rb ratio of 200:1. Later, Mejdahl (1987) and Huntley and Hancock (2001)
222 observed a linear relationship between Rb concentration and K concentration for multi-grain
223 K-feldspar extracts but with different slopes. Mejdahl (1987) looked at the concentrations of
224 bulk extracts whereas Huntley and Hancock (2001) corrected for the fact that the extracts

225 were not pure K-feldspar. Here we examined this relationship both at the intra-grain and the
226 inter-grain level. Finally, we compare our grain-averaged results with published values.

227
228 Figure 3a summarises a representative selection of repeat K and Rb concentration
229 measurements per grain (3 measurements per grain). It can be seen that in some grains the
230 repeat measurements are reproducible whereas in others there is considerable spread in either
231 or both axes (e.g. 133311_grain24, 981007_grain82). While it is true that the higher
232 concentrations of Rb are only found in high K grains, some high K grains contain very low
233 values of Rb.

234
235 The average single-grain Rb and K concentration results are presented in Fig. 3b. There is
236 significant variability in Rb (and K) concentration between individual grains and no clear
237 correlation between K and Rb is visible. Although the number of grains is limited, it is
238 interesting to note that none of the low K (<7%) IR-sensitive grains show high Rb
239 concentrations (>250 ppm). For the high K (>10%) grains, considerable variability (>15
240 times) in Rb concentration is observed between individual grains, even within the same
241 sample. For example, a single 200 μm K-feldspar grain of sample 178109 with K
242 concentration $10.6 \pm 0.3\%$ has a Rb concentration of 1478 ± 135 ppm. More than 35 % of the
243 internal beta dose rate for this grain is due to Rb assuming an internal U and Th contribution
244 of 0.1 Gy ka^{-1} (based on Mejdahl, 1987 and Zhao and Li, 2005). In contrast to this, another K-
245 feldspar grain from the same sample with a K concentration of $12.0 \pm 0.3\%$ and Rb
246 concentration of 88 ± 8 ppm, receives only 3% of the internal dose rate from Rb. The
247 contribution of Rb to the total dose rate for these two grains is ~20% and ~1%, respectively.
248 At least at the single-grain level, it may be that internal Rb variation between individual
249 grains contributes to D_e scatter in K-rich feldspar grains. Nevertheless, the observed D_e scatter

250 between individual feldspar grains in Fig. 1 cannot be explained by inter-grain Rb
251 concentration variation, because the predicted lines were derived using a fixed assumed Rb
252 concentration of 400 ppm. Had the actual Rb concentrations been significantly higher than
253 this, the predicted D_e relationship with K concentrations (dashed lines) would have been
254 incorrectly low, and the measured single-grain D_e estimates would have tended to lie above
255 the predicted line; this is not observed. And since the assumed 400 ppm Rb concentration
256 only contributes ~3% to the total dose rate, if the actual Rb concentrations were very much
257 smaller than assumed, the dose rate (and so the dose) compared to other grains would only be
258 3% different from the mean. We conclude that variations in Rb cannot account for the
259 absence of correlation of D_e with K concentration.

260

261 Figure 3c summarises our Rb data averaged over all grains for the Na- and K-feldspar rich
262 fractions together with published data. Our results are consistent with those reported earlier
263 although systematically slightly lower; this may be due to different geological source areas.
264 The average Rb concentration for feldspars with K concentration >10 % is 353 ± 20 ppm ($\sigma =$
265 131 ; $n=42$; cyan symbol), which is in good agreement with the value of 400 ± 100 ppm
266 suggested by Huntley and Hancock (2001). In our view, apart from the Mejdahl (1987) data,
267 any linear correlation between Rb and K concentration is rather weak. Because the data in
268 Mejdahl (1987) was obtained on bulk Na and K-rich feldspar fractions and no correction was
269 made for other mineral contamination, it is possible that his clear correlation was induced by
270 quartz contamination of the extracts (i.e. as a result of dilution).

271

272 5. Discussion and conclusions

273 It seems very likely that the emitted energy per disintegration and the half-life are sufficiently
274 well-known that the feldspar doses predicted in Figs. 1 and 2 do not suffer from significant

275 systematic error. Over a period of 26 years, the infinite matrix beta dose rate for ^{40}K has only
276 changed by 2.5 % (Aitken, 1985; Guérin et al., 2011). In addition, the grain size dependence
277 has been calculated at least by Mejdahl (1979) and Fain et al. (1999) and both gave very
278 similar results. Therefore, we can infer that inaccuracies in the attenuation of dose-rates to
279 different grain sizes cannot account for the unexpected relationships measured in this study.
280

281 The precision and accuracy of K analyses at the single-grain level have been demonstrated.
282 By measuring calibration standards we deduce that the μ -XRF analyses are accurate within
283 0.2–0.9 K % and reproducible within 0.1–0.47 K %. Repeated measurements on single-grains
284 extracted from sediment samples further show that the overall standard deviation in our
285 analysis of an individual grain (i.e. including natural variability in concentration within a
286 grain) is 0.8 % K. The corresponding value for the multi-grain XRF measurements is less than
287 0.4 % K (including any variability as a function of grain size between 40 μm and 500 μm).
288 In summary, we do not think that the discrepancies observed between observations and
289 predictions can be attributed to uncertainties in expected dose rates. They must be connected
290 in some way to the measurement of dose. It is important at this point to emphasize that our
291 dose estimates are all based on a quartz beta source calibration. This is standard practice
292 because the rate of energy absorption from both beta particles and gamma rays is
293 indistinguishable for quartz and feldspar. However, beta source calibration is undertaken by
294 matching the luminescence (L_γ) from a known gamma dose (D_γ) with the luminescence (L_β)
295 from an unknown beta dose (D_β). That is, $D_\gamma\chi_\gamma = D_\beta\chi_\beta$, where χ_γ and χ_β are the gamma and
296 beta luminescence sensitivities per unit dose. Thus, for the quartz dose rate to apply to
297 feldspar we must assume that the ratio χ_γ/χ_β is the same for both quartz and feldspar. Since
298 gamma rays and beta particles deposit energy by the same mechanism this ratio has been
299 assumed to be unity in both cases. This is an important assumption and we return to it below.

300

301 It is unlikely that we are unable to detect the expected correlations between dose and K
302 concentration or grain size because the grains are poorly bleached. Had this been the case, all
303 single grain dose analyses should lie above the predicted relationships in Fig. 1, at least on
304 average. Indeed, large aliquot K-feldspar D_e values (green) are in slightly better agreement
305 with the expected values and are, except for sample 133311 (Fig. 1d), systematically larger
306 than the CAM or synthetic aliquot single-grain K-feldspar D_e estimates.

307

308 Incomplete bleaching also seems unlikely to be an explanation for the discrepancies in the
309 multi-grain data presented in Fig. 2. First of all, the samples were chosen from environments
310 that were likely to be well-bleached with the possible exception of sample 133311 (Fig. 1d,
311 2e). In addition, in two cases the pIRIR relationship with grain size when extrapolated to zero
312 predicts a dose consistent with or below the observed quartz dose (Fig. 2a,e). For sample
313 178112 (Fig. 2c), it is difficult to draw such a conclusion because the total doses are very
314 small and a very-hard to bleach pIRIR component may play a role. However, the IR_{50} signal
315 is probably well-bleached and the linear relationships observed for pIRIR and IR_{50} would
316 require that any incomplete bleaching is independent of grain size. This is known not to be
317 true for quartz (Olley et al., 1998; Truelsen and Wallinga, 2003) and seems very unlikely for
318 feldspar. We are confident that incomplete bleaching can be dismissed as a significant
319 contributory factor to the discrepancies observed in Figs. 1 and 2.

320

321 Neudorf et al. (2012) also did not observe a correlation between D_e and single grain K
322 concentrations and they concluded that the primary cause of their considerable over-
323 dispersion was mixing of units of different age. We are confident that this explanation does
324 not apply to at least 4 out of 5 of our samples (see Section 2.1).

325
326 Fading is an obvious explanation for dose underestimation; fading rates as a function of grain
327 size are presented in Fig. S3. We first consider the standard large aliquot dose estimates for
328 ~200 μm diameter grains (Fig. 1). The large aliquot dose estimates are in fairly good
329 agreement with those expected for samples 981007, 178112 and (by extrapolation) D38146
330 (Fig. 1b,c; Fig. 2c,g) for which fading appears not to be a problem. On the other hand, the 200
331 μm large aliquot dose estimates for samples 178109 and 133311 significantly underestimate
332 the expected values by ~20 and ~30%, respectively. The average pIRIR fading rates at 200
333 μm are 2%/decade and 1.3%/decade respectively and thus only able to potentially explain the
334 large aliquot underestimate for sample 178109; for 133311 the fading rate is too low.
335
336 No significant trend in IR_{50} or pIRIR g values with grain size is observed in our samples,
337 except for the IR_{50} signal of sample 178112 for which there seems to be a positive correlation
338 (Fig. S3). We now turn to the isochron data of Fig. 2. Given that fading appears to be
339 independent of grain-size, one would expect to see pIRIR data parallel to the expected
340 feldspar dose dependence and intersecting the y-axis below the quartz dose. This is not
341 observed in Fig. 2. If, instead, fading were to be grain size dependent then it might have been
342 possible to explain the observed data in Fig. 2e (133311 for which all data lie below the
343 expected line). However, neither IR_{50} nor pIRIR₁₅₀ fading data show a correlation with grain
344 size for this sample. Differential fading may explain the data of sample 178112 (Fig. 2c), but
345 only if a residual dose is subtracted from all dose values. On the other hand, grain size
346 dependent fading is unlikely to explain the data in of 178109 (Fig. 2a) and cannot explain the
347 data of sample D38146 (Fig. 2g). In the first case such an explanation would require that
348 fading is negligible for very small grain sizes and very large at 400 μm (which is not observed
349 in Fig. S3). In the second case, fading cannot explain the dose overestimates.

350

351 It is also difficult to explain the lack of correlation between single grain D_e and K
352 concentration (Fig. 1) in terms of differential fading between individual low and high K
353 grains. In samples 178112 and 133311, the pIRIR D_e values recorded by the low K grains are
354 either consistent with or above the predicted relationship; this implies that the pIRIR signal of
355 low K grains is essentially stable. In contrast, that of high K grains must be very unstable
356 because the high K doses lie considerably below the expected line. Published fading rates for
357 the blue violet emission from alkali-feldspars do not suggest such a correlation (e.g. Huntley
358 and Lian, 2006; Barré and Lamothe, 2010). Furthermore, published feldspar single grain
359 studies do not find any correlation between g value and K content (e.g. Neudorf et al., 2012;
360 Trauerstein et al., 2014).

361

362 In summary, it has again proved impossible to observe the expected correlation between D_e
363 and K concentration (and grain size) even in low dose rate environments (down to $0.94 \text{ Gy}\cdot\text{ka}^{-1}$
364 external dose rate, 178112, Fig. 1c and 2c) where the internal dose rate contributes up to 50
365 % of the total. We have demonstrated that our K analyses are precise and accurate and that it
366 is unlikely that a grain-size-dependence on phenomena such as incomplete resetting or signal
367 instability can explain these results. We also dismiss post-depositional mixing as a potential
368 cause in at least 4 out of 5 samples. It is deduced that the absence of correlation must be
369 related to dose measurement using feldspar luminescence. Recent work by Hansen et al.
370 (these proceedings) has shown that the beta to gamma dose rate ratio measured using
371 luminescence is 15 % different for quartz and feldspar. This discrepancy must arise from
372 differences in quartz OSL and feldspar pIRIR response to β and γ radiation, i.e. the ratio
373 χ_γ/χ_β referred to above is different for quartz and feldspar, at least for these samples. We
374 hypothesise that this phenomenon also exists both between individual feldspar grains and

375 between grains of different sizes, and that this is at least part of the cause of the lack of
376 correlations. Until these problems are resolved it would be unwise, in our view, to interpret
377 single-grain feldspar dose distribution in terms of any extrinsic phenomena.

378

379 **Acknowledgements**

380 J.-P. Buylaert and G. Újvári received funding from the European Research Council (ERC)
381 under the European Union Horizon 2020 research and innovation programme ERC-2014-StG
382 639904 – RELOS. We thank Pedro Cunha and Antonio Martins for the Portuguese samples
383 and Marie Fibæk for the Skagen sample. We are grateful to Louise Helsted for help with
384 sample preparation.

385

386 **References**

- 387 Aitken, M.J., 1985. Thermoluminescence Dating. Academic Press, London.
- 388 Auclair, M., Lamothe, M., Huot, S., 2003. Measurement of anomalous fading for feldspar
389 IRSL using SAR. *Radiat. Meas.* 37, 487-492.
- 390 Barré, M., Lamothe, M., 2010. Luminescence dating of archaeosediments: A comparison of
391 K-feldspar and plagioclase IRSL ages. *Quat. Geochronol.* 5, 324–328.
- 392 Buylaert, J.P., Thiel, C., Murray, A.S., Vandenberghe, D., Yi, S., Lu, H., 2011. IRSL and
393 post-IR IRSL residual doses recorded in modern dust samples from the Chinese Loess
394 Plateau. *Geochronometria* 38, 432–440.
- 395 Buylaert, J.P., Jain, M., Murray, A.S., Thomsen, K.J., Thiel, C., Sohbati, R., 2012. A robust
396 feldspar luminescence dating method for Middle and Late Pleistocene sediments. *Boreas* 41,
397 435-451.

- 398 Bøtter-Jensen, L., Andersen, C.E., Duller, G.A.T., Murray, A.S., 2003. Developments in
399 radiation, stimulation and observation facilities in luminescence measurements. *Radiat. Meas.*
400 37, 535–541.
- 401 Bøtter-Jensen, L., Thomsen, K.J., Jain, M., 2010. Review of optically stimulated
402 luminescence (OSL) instrumental developments for retrospective dosimetry. *Radiat. Meas.*
403 45, 253–257.
- 404 Duller, G.A.T., 2016. *Analyst v.4.31.9: User Manual*. Aberystwyth Luminescence Research
405 Laboratory, Aberystwyth University, pp. 1-83.
- 406 Fain, J., Soumana, S., Montret, M., Miallier, D., Pilleyre, T., Sanzelle, S., 1999. TL and ESR
407 dating: beta-dose attenuation for various grain shapes calculated by a Monte-Carlo method.
408 *Quater. Geochronol.* 18, 231–234.
- 409 Galbraith, R., Roberts, R.G., Laslette, G., Yoshidha, Olley, J., 1999. Optical dating of single
410 and multiple grain quartz from Jinmium Rock Shelter, Northern Australia. Part I,
411 experimental design and statistical models. *Archaeometry* 41, 339-364.
- 412 Guérin, G., Mercier, N., Adamiec, C., 2011. Dose-rate conversion factors: update. *Ancient TL*
413 29, 5–8.
- 414 Hansen, V., Murray, A.S., Thomsen, K.J., Jain, M., Autzen, M., Buylaert, J.-P., Towards
415 understanding the origins of over-dispersion in beta source calibration. *Radiat. Meas.*, these
416 proceedings.
- 417 Huntley, D. J., Baril, M. R., 1997. The K content of the K-feldspars being measured in optical
418 dating or in thermoluminescence dating. *Ancient TL* 15, 11–13.
- 419 Huntley, D.J., Hancock, R.G.V., 2001. The Rb contents of the K-feldspar grains being
420 measured in optical dating. *Ancient TL* 19, 43–46.
- 421 Huntley, D.J., Lian, O.B., 2006. Some observations on tunnelling of trapped electrons in
422 feldspars and their implications for optical dating. *Quat. Sci. Rev.* 25, 2503–2512.

- 423 Jochum, K.P., Nohl, U., Herwig, K., Lammel, E., Stoll, B., Hofmann, A.W., 2005. GeoReM:
424 a new geochemical database for reference materials and isotopic standards. *Geostand.*
425 *Geoanal. Res.* 29, 333–338.
- 426 Kook, M.H., Lapp, T., Murray, A.S., Thiel, C., 2012. A Risø XRF attachment for major
427 element analysis of aliquots of quartz and feldspar separates, 2012. UK Luminescence and
428 ESR Meeting, Aberystwyth, September 2012 (abstract), p. 37.
- 429 Li, B., Li, S-H., Wintle, A.G., Zhao, H., 2008. Isochron dating of sediments using
430 luminescence of K-feldspar grains. *J. Geophys. Res.* 113, F02026.
- 431 Madsen, A.T., Buylaert, J.-P., Murray, A.S., 2011. Luminescence dating of young coastal
432 deposits from New Zealand using feldspar. *Geochronometria* 38, 379–390.
- 433 Mejdahl, V., 1979. Thermoluminescence Dating: Beta-Dose Attenuation in Quartz Grains.
434 *Archaeometry* 21, 61-72.
- 435 Mejdahl, V., 1983. Feldspar inclusion dating of ceramics and burnt stones. *European PACT J.*
436 9, 351-364.
- 437 Mejdahl, V., 1987. Internal radioactivity in quartz and feldspar grains. *Ancient TL* 5, 10-17.
- 438 Murray, A.S, Funder, S., 2003. Optically stimulated luminescence dating of a Danish Eemian
439 coastal marine deposit: a test of accuracy *Quat. Sci. Rev.* 22, 1177-1183.
- 440 Neudorf, C.M., Roberts, R.G., Jacobs, Z., 2012. Sources of overdispersion in a K-rich
441 feldspar sample from north-central India: insights from De, K content and IRSL age
442 distributions for individual grains. *Radiat. Meas.* 47, 696–702.
- 443 Olley, J., Caitcheon, G., Murray, A., 1998. The distribution of apparent dose as determined by
444 optically stimulated luminescence in small aliquots of fluvial quartz: implications for dating
445 young sediments. *Quat. Sci. Rev.* 17, 1033–1040.

- 446 Porat, N., Faerstein, G., Medialdea, A., Murray, A.S., 2015. Re-examination of common
447 extraction and purification methods of quartz and feldspar for luminescence dating. *Ancient*
448 *TL* 33, 22–30.
- 449 Smedley, R.K., Pearce, N.J.G., 2016. Internal U, Th and Rb concentrations of alkali-feldspar
450 grains: Implications for luminescence dating. *Quat. Geochronol.* 35, 16-25.
- 451 Thiel, C., Buylaert, J.-P., Murray, A.S., Terhorst, B., Hofer, I., Tsukamoto, S., Frechen, M.,
452 2011. Luminescence dating of the Stratzing loess profile (Austria) – Testing the potential of
453 an elevated temperature post-IR IRSL protocol. *Quat. Int.* 234, 23–31.
- 454 Thomsen, K.J., Murray, A.S., Bøtter-Jensen, L., 2005. Sources of variability in OSL dose
455 measurements using single grains of quartz. *Radiat. Meas.* 39, 47-61.
- 456 Thomsen, K.J., Murray, A.S., Jain, M., Bøtter-Jensen, L., 2008. Laboratory fading rates of
457 various luminescence signals from feldspar-rich sediment extracts. *Radiat. Meas.* 43,
458 1474–1486.
- 459 Thomsen, K.J., Murray, A.S., Jain, M., 2012. The dose dependency of the overdispersion
460 of quartz OSL single grain dose distributions. *Radiat. Meas.* 47, 732-739.
- 461 Thomsen, K.J., Murray, A.S., Buylaert, J.P., Jain, M., Hansen, J.H., Aubry, T., 2016. Testing
462 single-grain quartz OSL methods using sediment samples with independent age control from
463 the Bordes-Fitte rockshelter (Roches d'Abilly site, Central France). *Quat. Geochronol.* 31, 77-
464 96.
- 465 Trauerstein, M., Lowick, S.E., Preusser, F., Schlunegger, F., 2014. Small aliquot and single
466 grain IRSL and post-IR IRSL dating of fluvial and alluvial sediments from the Pativilca val-
467 ley, Peru. *Quat. Geochron.* 22, 163-174.
- 468 Truelsen, J.L., Wallinga, J., 2003. Zeroing of the OSL signal as a function of grain size:
469 investigating bleaching and thermal transfer for a young fluvial sample. *Geochronometria*, 22,
470 1–8.

471 Warren, S.E., 1978. Thermoluminescence dating of pottery: an assessment of the dose-rate
472 from rubidium. *Archaeometry* 20, 69–70.

473 Willerslev, E., Cappellini, E., Boomsma, et al., 2007. Ancient biomolecules from deep ice
474 cores reveal a forested southern Greenland. *Science* 317, 111-114.

475 Zhao, H., Li, S.-H. 2005. Internal dose rate to K-feldspar grains from radioactive elements
476 other than potassium. *Radiat. Meas.* 40, 84–93.

477

478 **Figure captions**

479

480 Fig. 1 a-d. Single-grain pIRIR D_e as a function of average K concentration per grain for four
481 different samples. Grains from the Na-feldspar extract (NaF) have red symbols and those
482 from K-feldspar extract (KF) are shown in black. Large aliquot (quartz=blue; K-
483 feldspar=green) results, synthetic aliquots from KF single grain data (white), Central Age
484 Model (Galbraith et al., 1999; CAM) single grain K and D_e results (cyan) and predicted
485 feldspar dose (grey dashed line) are also shown. The large aliquot and synthetic aliquot KF
486 D_e 's are plotted at the K concentration measured using the multi-grain XRF-attachment. The
487 predicted feldspar line was calculated from the quartz age and calculated feldspar dose rate
488 for different K concentrations. Uncertainties on both axes represent one standard error. Note
489 that 9 out 229 grains have K values significantly greater than 14%. We attribute this to
490 experimental uncertainty, possibly arising from self- absorption geometry effects in the μ -XRF
491 measurements; pressed powders used for calibration had flat surfaces whereas single grains
492 had irregular surfaces.

493

494 Fig. 2 a-h. Multi-grain isochron plots (both IR₅₀ and pIRIR) and corresponding XRF analyses
495 for the different K-feldspar grain size extracts for three samples presented in Fig.1 and one

496 additional Chinese loess sample (D38146). Predicted lines (dashed) are calculated from the
497 quartz D_e (pink), beta attenuation factors (Mejdahl, 1979) and an assumed K concentration of
498 12.5% and a Rb concentration of 400 ppm.

499

500 Fig. 3 a) Representative Rb versus K plots for individual feldspar grains (3 measurement per
501 grain). b) Summary of individual grain Rb and K data for all measured grains (n=202). Colour
502 codes identify feldspar density fractions (red=Na-separate, black=K-separate). c) Same data
503 as in b) but now averaged over all the grains in the Na- and K-feldspar extracts, together with
504 published data. The average of all the samples with K concentration >10% is also plotted
505 (cyan symbol). Uncertainties represent one standard error for both axes in b) and c).

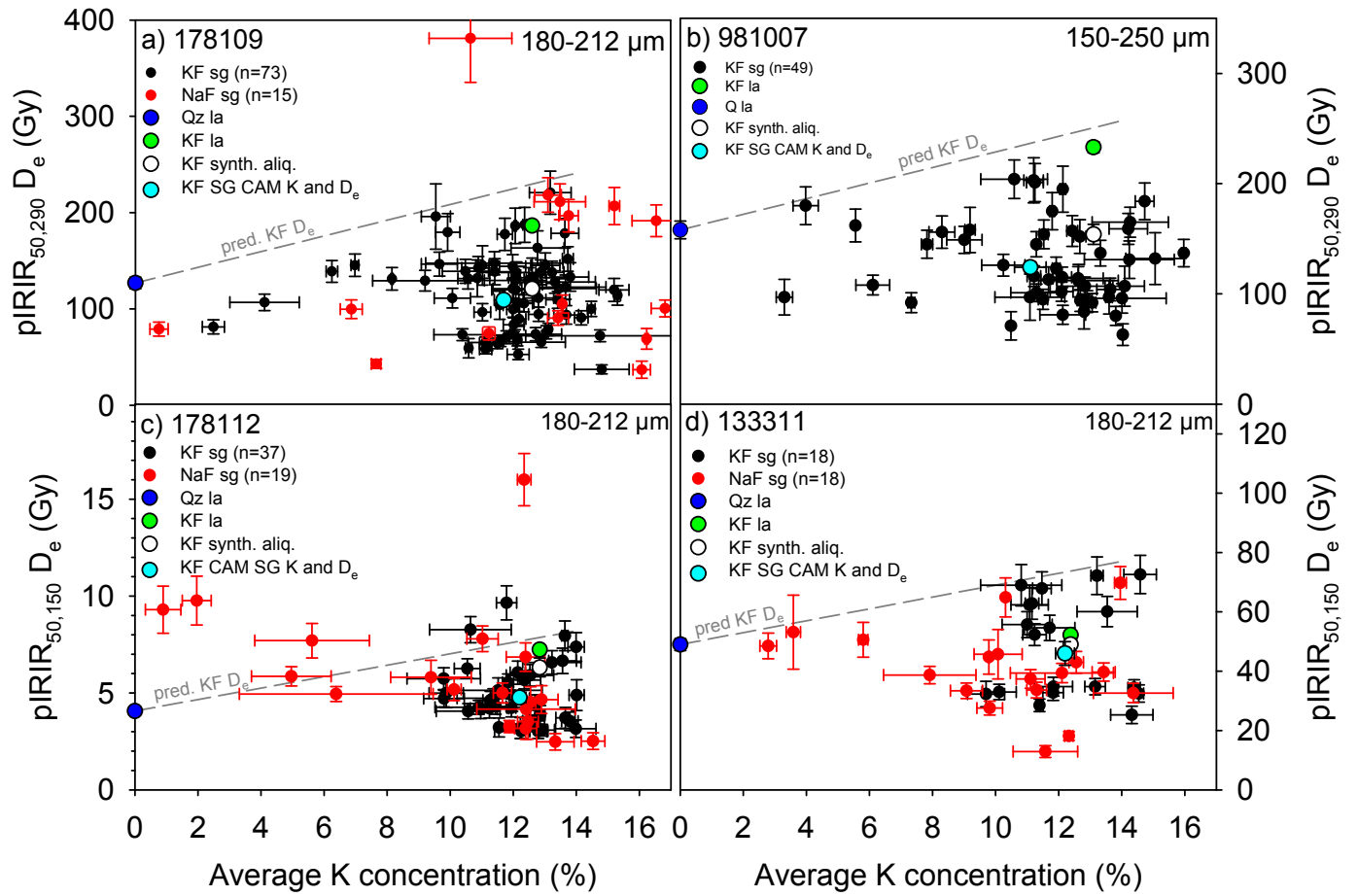


Fig. 1

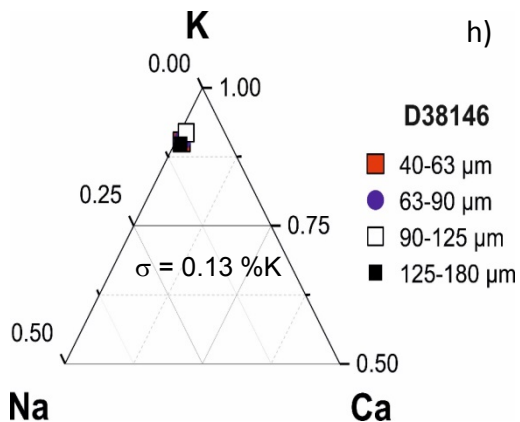
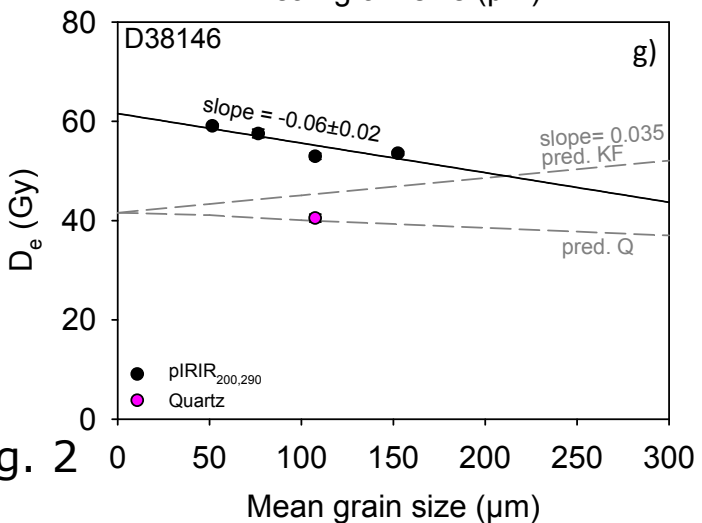
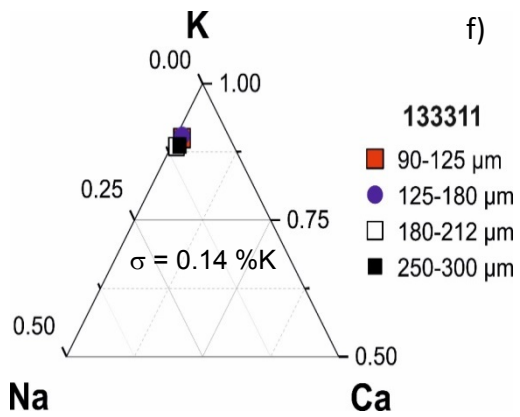
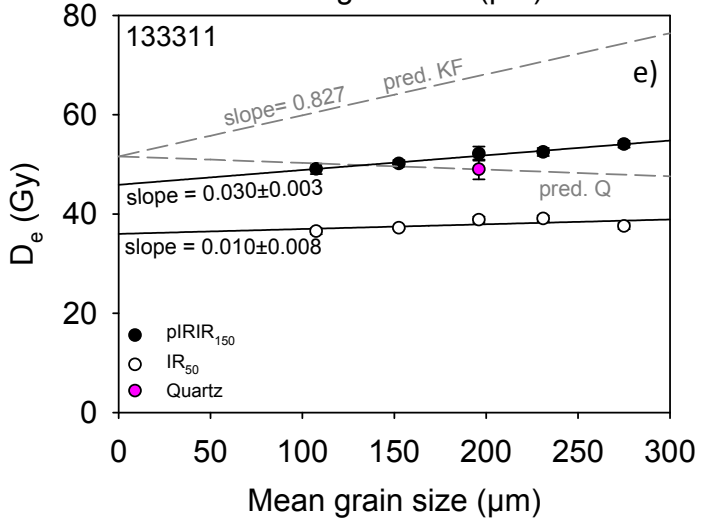
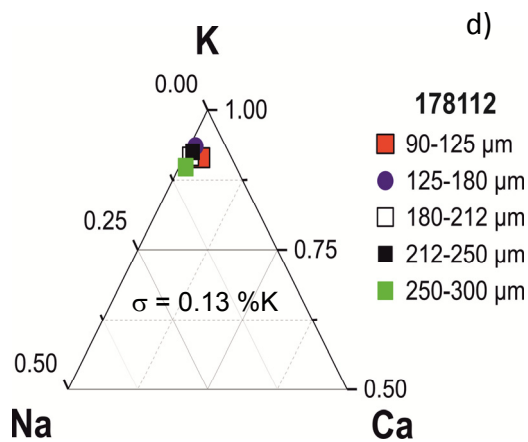
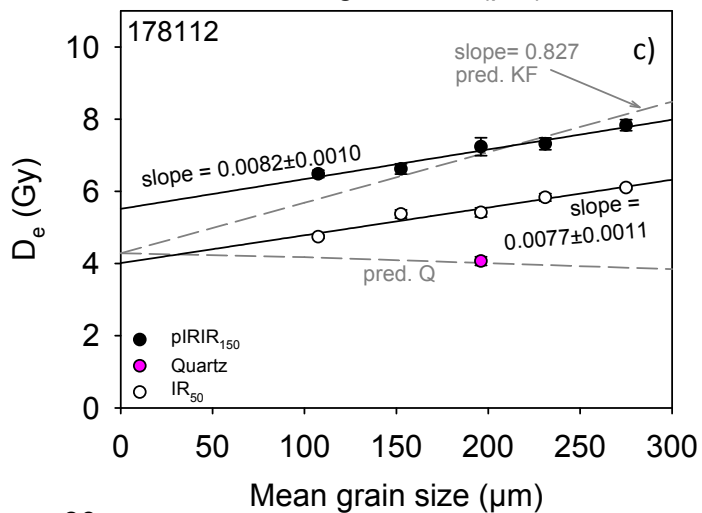
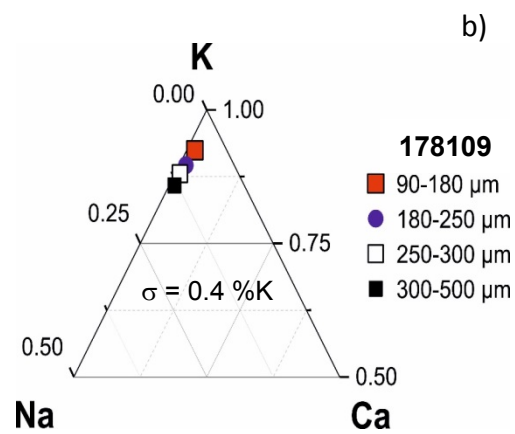
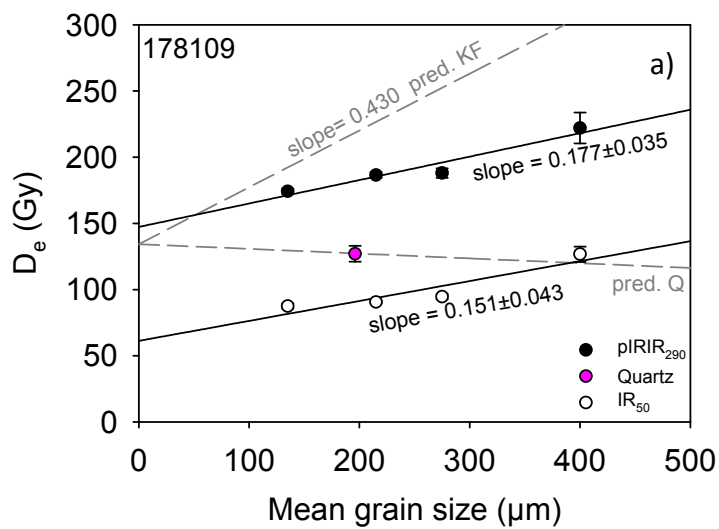


Fig. 2

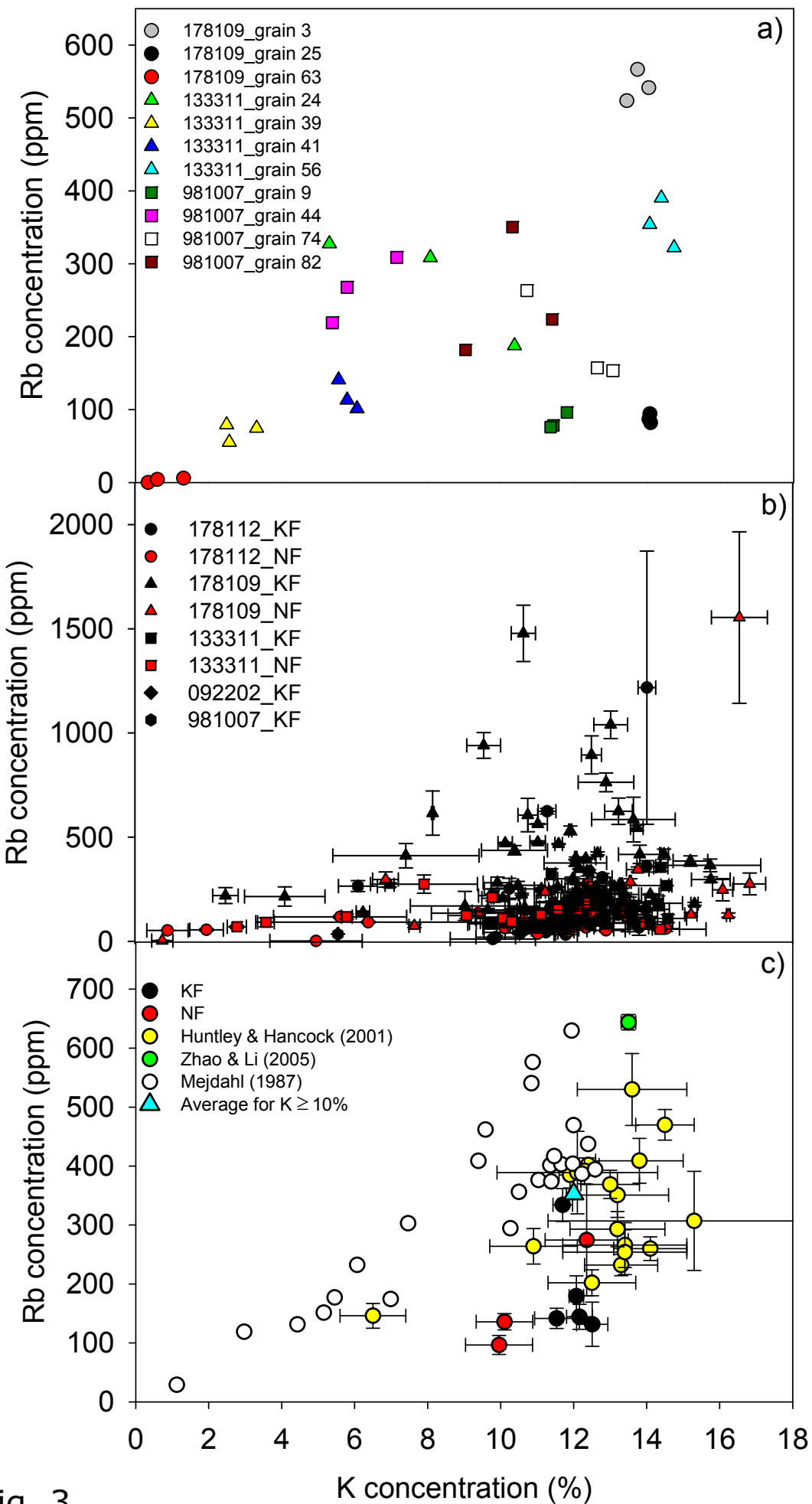


Fig. 3

K concentration (%)

Highlights:

- Unable to establish any correlation between single-grain pIRIR D_e and K concentration, even in feldspar grains for which the internal dose rate should dominate
- Slopes of IR₅₀ and pIRIR isochrons (D_e as a function of grain size) not consistent with model predictions
- Rb content in individual feldspar grains highly variable